

논문 2011-06-18

# Intelligent Technique Application for Autonomous Lateral Position Control of an Unmanned 4 Wheel Steered Snowplow Robotic Vehicle

Seul Jung\*, T. C. Hsia

**Abstract :** This paper presents an intelligent control approach for lateral position control of an autonomous four wheel steered snowplowing robotic vehicle. The vehicle is built for removing snow on the highway. Dynamics of the vehicle is derived and linearized for LQR control. Lateral position is controlled by the LQR method first, then the neural network control technique is introduced to improve tracking performances under the presence of load. The feasibility of using four wheel steering control is investigated by simulation studies of lateral position tracking of the Ford F-250 truck model. Performances of a LQR control method and a neural network control method under virtual snowplowing situation are compared.

**Keywords :** Neural network, LQR, Lateral control, Highway snowplowing vehicle

## 1. Introduction

Automation of highway maintenance robotic vehicles is demanded for safety of workers on the road. Research on automation of crack sealing vehicle and a snowplow vehicle is rapidly increased and developed.

Automation of the snowplow vehicle is desired where a driver of the snowplow vehicle cannot see the guard rail covered with snow as shown in Fig. 1. The guard rail is often used as the reference of following road. Driving under unseen guard rail situation may lead to a deadly accident if the vehicle hits the guard rail hidden under snow pile.

Research on automation of highway

maintenance vehicles has been initiated by the CALTRAN in California, USA. The autonomous highway management and construction technology (AHMCT) center at UC Davis is one of the leading research groups that conduct research on heavy duty field robotic vehicle projects. Several vehicles have already developed and utilized [1]. Similar research has also been conducted in Korea [2].

Automatic steering control of the vehicle is required for autonomous maneuvering along with GPS localization, GIS analysis, and sensor implementation.



Fig. 1. CALTRAN's snowplow vehicle

---

\* Corresponding Author

Manuscript received : 2011. 02. 11.,

Revised : 2011. 03. 15.,

Accepted : 2011. 04. 04.

Seul Jung : Chungnam National University

T. C. Hsia : University of California, Davis

※ This research has been partially supported by Korea Research Foundation in 2010.

The ultimate goal of this research is to develop the semi-autonomous snowplowing

vehicle that can follow the guard rail of the highway without collision. This requires accurate lateral control of the vehicle by maintaining a constant distance from the guard rail based on sensing information.

Active research on lateral control of the vehicles such as the  $H_\infty$  control and the yaw rate feedback control has been presented [3-5]. Experimental studies of robust lateral control of a highway vehicle have been conducted [6,7]. Fuzzy control has been implemented for steering control [8,9].

In this paper, the feasibility of using four wheel steering control is investigated. As an extension of our previous research, a four wheeled vehicle is modelled and controlled. The LQR control method is used to obtain optimal controllers' gains for linearized model under load presence.

A neural network controller is introduced to compensate for disturbance rejection. Neural network is known as a powerful nonlinear controller and successful applications can be found [10-13].

Simulation studies are conducted for a Ford F-250 truck model and position tracking performances are compared under the virtual plowing condition.

## II. Four Wheel Steered Vehicle Dynamics

The vehicle is steered by both the front and the rear wheel [14].

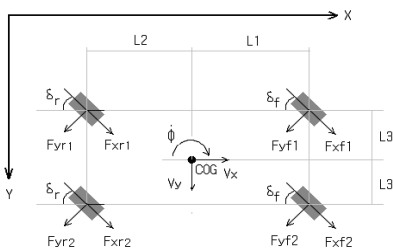


Fig. 2. Model of 4 wheel steering vehicle  
X axis :

$$m(\dot{V}_x - V_y \omega) = F_{yf1} \cos \delta_f - F_{yf1} \sin \delta_f + F_{yf2} \cos \delta_f - F_{yf2} \sin \delta_f + F_{xr1} \cos \delta_r - F_{yr1} \sin \delta_r + F_{xr2} \cos \delta_r - F_{yr2} \sin \delta_r$$

Y axis

$$m(\dot{V}_y + V_x \omega) = F_{yf1} \sin \delta_f + F_{yf1} \cos \delta_f + F_{yf2} \sin \delta_f + F_{yf2} \cos \delta_f + F_{xr1} \sin \delta_r + F_{yr1} \cos \delta_r + F_{xr2} \sin \delta_r + F_{yr2} \cos \delta_r$$

Z axis

$$I_z \ddot{\phi} = (L_1 \sin \delta_f + L_3 \cos \delta_f) F_{yf1} + (L_1 \cos \delta_f - L_3 \sin \delta_f) F_{yf1} + (L_1 \sin \delta_f - L_3 \cos \delta_f) F_{yf2} + (L_1 \cos \delta_f + L_3 \sin \delta_f) F_{yf2} + (-L_2 \sin \delta_r + L_3 \cos \delta_r) F_{xr1} + (-L_2 \cos \delta_r - L_3 \sin \delta_r) F_{yr1} + (-L_2 \sin \delta_r - L_3 \cos \delta_r) F_{xr2} + (-L_2 \cos \delta_r + L_3 \sin \delta_r) F_{yr2} \quad (1)$$

where  $m$  is a total mass of the vehicle,  $\phi$  is a yaw angle,  $\delta_f$  is a steering angle of the front wheel,  $\delta_r$  is a steering angle of the rear wheel,  $L_1$  is the distance from the center of the front wheel to COG,  $L_2$  is the distance from the center of the rear wheel to COG,  $V_x$  is a velocity of the vehicle along  $x$  direction,  $V_y$  is a velocity of the vehicle along  $y$  direction,  $F_{xf}$  is a longitudinal force of the front wheel along  $x$  direction,  $F_{xr}$  is a longitudinal force of the rear wheel along  $x$  direction,  $F_{yf}$  is lateral force of the front wheel along  $y$  direction,  $F_{yr}$  is a lateral force of the rear wheel along  $y$  direction,  $I_z$  is yaw moment of inertia along  $z$  direction.

Slip angles are defined by

$$\alpha_{f1} = \delta_f - \frac{V_x + L_3 \dot{\phi}}{V_y + L_1 \dot{\phi}}, \quad \alpha_{f2} = \delta_f - \frac{V_x - L_3 \dot{\phi}}{V_y + L_1 \dot{\phi}},$$

$$\alpha_{r1} = \delta_r - \frac{V_x + L_3 \dot{\phi}}{V_y - L_2 \dot{\phi}}, \quad \alpha_{r2} = \delta_r - \frac{V_x - L_3 \dot{\phi}}{V_y - L_2 \dot{\phi}} \quad (2)$$

For simplicity, the vehicle is assumed to be symmetrical and its dynamics is considered as a bicycle model as shown in Fig. 3.

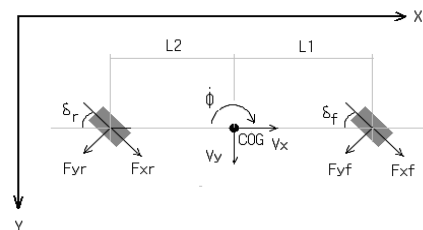


Fig. 3. Bicycle model of 4 wheel steered vehicle

The dynamic equations for the bicycle model are derived based on the references [14,15].

$$\begin{aligned} m(\dot{V}_x - V_y \dot{\phi}) &= F_{xf} \cos \delta_f + F_{xr} \cos \delta_r - F_{yf} \sin \delta_f + F_{yr} \sin \delta_r \\ m(\dot{V}_y + V_x \dot{\phi}) &= F_{yf} \cos \delta_f + F_{yr} \cos \delta_r + F_{xf} \sin \delta_f - F_{xr} \sin \delta_r \\ I_z \ddot{\phi} &= L_1 F_{yf} \cos \delta_f - L_2 F_{yr} \cos \delta_r + L_1 F_{xf} \sin \delta_f + L_2 F_{xr} \sin \delta_r \end{aligned} \quad (3)$$

Slip angles are simplified as

$$\alpha_f = \delta_f - \frac{L_1 \dot{\phi} + V_y}{V_x}, \alpha_r = \delta_r - \frac{v_y - L_2 \dot{\phi}}{V_x} \quad (4)$$

where  $\alpha_f$  is a slip angle of the front wheel and  $\alpha_r$  is a slip angle of the rear wheel. Lateral forces are defined as

$$F_{yf} = 2C_{\alpha f} \alpha_f, F_{yr} = 2C_{\alpha r} \alpha_r \quad (5)$$

where  $C_{\alpha f}$  and  $C_{\alpha r}$  are cornering stiffness.

Under the assumption that the vehicle is moving at a constant velocity in longitudinal direction and the steer angle  $\alpha_f$  is small. A steering angle is considered as a control input, and a yaw angle  $\phi$  and a lateral position  $y$  are outputs to be controlled.

Let  $\omega = \dot{\phi}$  and combining equations (3), (4), and (5) yields a MIMO system that has the state space representation as

$$\begin{bmatrix} \dot{V}_y \\ \dot{\omega} \end{bmatrix} = \begin{bmatrix} -\frac{a_2}{m} & -(V_x + \frac{a_1}{m}) \\ -\frac{a_1}{I_z} & -\frac{a_3}{I_z} \end{bmatrix} \begin{bmatrix} V_y \\ \omega \end{bmatrix} + \begin{bmatrix} \frac{2C_{\alpha f}}{m} & \frac{2C_{\alpha r}}{m} \\ \frac{2L_1 C_{\alpha f}}{I_z} & -\frac{2L_2 C_{\alpha r}}{I_z} \end{bmatrix} \begin{bmatrix} \delta_f \\ \delta_r \end{bmatrix} \quad (6)$$

where

$$a_1 = \frac{2L_1 C_{\alpha f} - 2L_2 C_{\alpha r}}{V_x}, a_2 = \frac{2C_{\alpha f} + 2C_{\alpha r}}{V_x}, a_3 = \frac{2L_1^2 C_{\alpha f} + 2L_2^2 C_{\alpha r}}{V_x}$$

### III. LQR Control for Lateral Position

A LQR control block diagram for lateral position is shown in Fig. 4. The goal of the LQR control is to minimize the following objective function

$$J = \int_0^{\infty} (x^T Q x + u^T R u) dt \quad (7)$$

where  $Q, R$  are the weighting matrices.  $Q, R$  values are selected based on trial and error process. The ultimate goal is to control the lateral position  $y$ .

The lateral position error is formed as

$$e_y = y_d - y \quad (8)$$

The yaw angle is formed as

$$e_\phi = \phi_d - \phi \quad (9)$$

Those errors are multiplied by LQR controller gains. The controller outputs for the front steering  $u_f$  and the rear steering  $u_r$  are defined as

$$u_y = k_{y_f} e_y + k_{y_\phi} e_\phi, u_r = k_{r_y} e_y + k_{r_\phi} e_\phi \quad (10)$$

where  $k_{y_f}, k_{y_\phi}, k_{r_y}, k_{r_\phi}$  are controller gains obtained by LQR method.

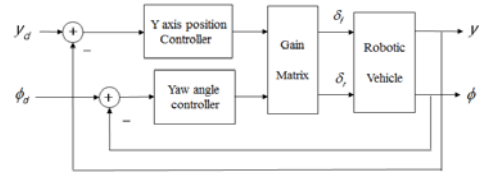


Fig. 4. Lateral control block diagram

For simplicity, we have the relationship  $\delta = u$  by not considering any dynamics of a steering actuator.

## IV. Neural Network Control

### 1. Neural network control structure

Here a neural network (NN) compensates for uncertainties by minimizing the errors defined in (10). The objective function is minimized in on-line fashion by adding compensating signal

from neural network to LQR controllers' output [4].

A control inputs are defined by adding neural network outputs  $u_N$  to (10) as

$$\delta_f = u_f + u_{NF} , \delta_r = u_\phi + u_{Nr} \quad (11)$$

where  $u_{Nf}, u_{Nr}$  are neural network outputs.

Fig. 5 shows the neural network control block diagram. At each sampling time, weights of neural network are updated to generate new compensating signals. The key issue here is how to implement on-line learning and control. To achieve on-line control, certain computing power is required for parallel processing.

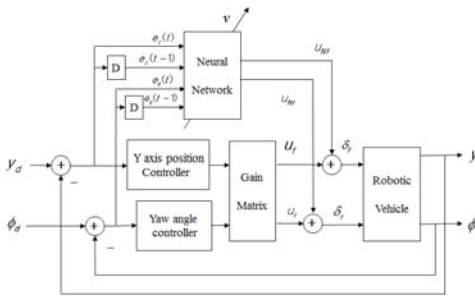


Fig. 5. Neural network control block diagram

## 2. Neural network learning

A general feed-forward structure has an input layer, a hidden layer, and an output layer as shown in Fig. 6. For the control application, 4 input buffers, 6 hidden units and 2 output units are used.

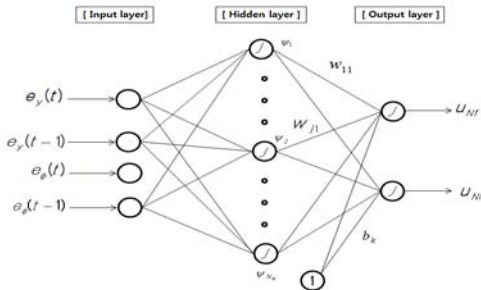


Fig. 6. Neural network structure

For a nonlinear function at a hidden layer

and an output layer we have used the hyperbolic tangent function as

$$\psi(x) = \frac{1 - e^{-x}}{1 + e^{-x}} \quad (12)$$

Since on-line learning and control is preferred, selecting training signals is very important. Typically, the bicycle model is a square MIMO system that two control inputs has to satisfy two different outputs simultaneously.

If  $f(y, \dot{y}, \ddot{y}, \phi, \dot{\phi}, \ddot{\phi}, \delta)$  is the system dynamics, equation (8), (10) and (11) can be represented as follows:

$$Ke = f - u_N \quad (13)$$

where  $K = \begin{bmatrix} k_{f_y} & k_{f_\phi} \\ k_{r_y} & k_{r_\phi} \end{bmatrix}$ ,  $e = [e_y, e_\phi]^T$ ,  $u_N = [u_{Nf}, u_{Nr}]^T$  and  $f = [f_y, f_r]^T$ .

So the training signal of neural network as the sum of outputs of PD controllers is defined as

$$v = Ke \quad (14)$$

where  $v = [v_y, v_r]^T$ .

The objective function is defined as

$$E = \frac{1}{2} v^T v \quad (15)$$

Differentiating (15) with respect to the weight  $w$ , we have

$$\frac{\partial E}{\partial w} = - \left[ \frac{\partial u_N}{\partial w} \right]^T v \quad (16)$$

The update equation in back propagation algorithm is

$$\Delta w(t) = \eta \left[ \frac{\partial u_N}{\partial w} \right]^T v + \alpha \Delta w(t-1) \quad (17)$$

$$w(t+1) = w(t) + \Delta w(t) \quad (18)$$

where  $\eta$  is a learning rate and  $\alpha$  is a momentum coefficient.

## V. Simulation Studies

1. Vehicle model

The following parameters of the vehicle are used for simulation studies.

Table 1. Parameters of 1985 Ford F-250

m	Iz	Cf, Cr	L1	L2
5760	5860	9000	4.76	6.35
lb	(lb · ft/sec <sup>2</sup> )	(lb/rad)	ft	ft
2612.6	810.2	4082.3	1.45	1.935
Kg	(Kg · m/sec <sup>2</sup> )	(Kg/rad)	m	m

Under the assumption of the constant longitudinal velocity, the state space representation of (6) becomes

$$\begin{bmatrix} \dot{V}_y \\ \dot{\omega} \end{bmatrix} = \begin{bmatrix} -0.625 & -9.5030 \\ 0.4884 & -19.3453 \end{bmatrix} \begin{bmatrix} V_y \\ \omega \end{bmatrix} + \begin{bmatrix} 3.125 & 3.125 \\ 14.6212 & -19.5051 \end{bmatrix} \begin{bmatrix} \delta_f \\ \delta_r \end{bmatrix} \quad (19)$$

LQR controller gains are selected from (19). However, the robotic vehicle model described in (1) is used for the simulation model instead of using (19).

2. LQR control

Different tracking responses of selecting gains as  $Q = \begin{bmatrix} 1 & 0 \\ 0 & 1 \end{bmatrix}$  and  $R = \begin{bmatrix} r & 0 \\ 0 & r \end{bmatrix}$  are tested and their results are plotted in Fig. 7. We see that the large value of  $r$  gives the good transient performance in the aspect of overshoot and settling time before 15 seconds. But when load (5000lb.ft/sec<sup>2</sup>) is present after 15 seconds, tracking performance became the worst.

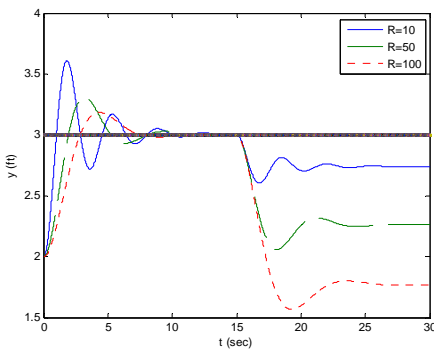


Fig. 7. Lateral control by LQR controllers

We also altered the value of Q matrix, but

$Q=I$  is found to be the best. We found that the value of Q matrix is more sensitive than that of R. Small change in Q results in bad tracking performances. Since the system is coupled, gain change affects tracking performances of both the position and the yaw angle.

Fig. 8 shows the tracking result when  $R=I$ , which shows a larger overshoot. The best tracking performance among several selections of R can be obtained when  $Q = \begin{bmatrix} 1 & 0 \\ 0 & 1 \end{bmatrix}$  and  $R = \begin{bmatrix} 10 & 0 \\ 0 & 10 \end{bmatrix}$ . At that time, we have found the controller gains as  $K = \begin{bmatrix} -0.0568 & 0.0636 \\ 0.2437 & -0.1491 \end{bmatrix}$ .

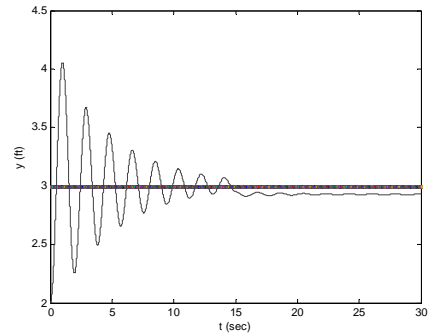


Fig. 8. Lateral position by LQR when R=I

Next test is to compare results between two and four wheel steered vehicles under the same condition. We see here from Fig 9. that both cases show tracking errors when load is present. However, a four wheel steering vehicle shows less error although a two wheel steered vehicle shows no overshoot at a transient response.

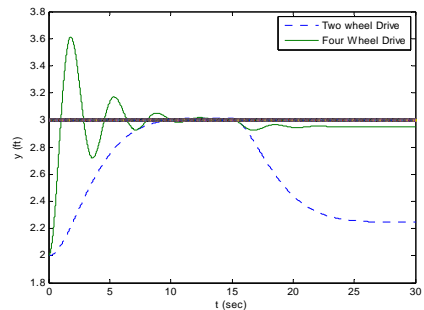


Fig. 9. Lateral position tracking results of two and four wheel steered vehicles

The plot explains that the system is much coupled so that optimized controller gains for  $\delta_f$  may not be optimal for both  $\delta_f$  and  $\delta_r$ .

### 3. Neural network control

3.1 Load is  $1000\text{ lb} \cdot \text{ft}/\text{sec}^2(138.2573\text{N})$ .

To minimize those tracking errors, the same simulation has been conducted by adding a neural network controller. For the neural network parameters,  $\eta = 0.000055, \alpha = 0.9$  are used and those values are optimized by trial and error basis. Fig.10 shows the lateral position tracking results for LQR control and neural network control.

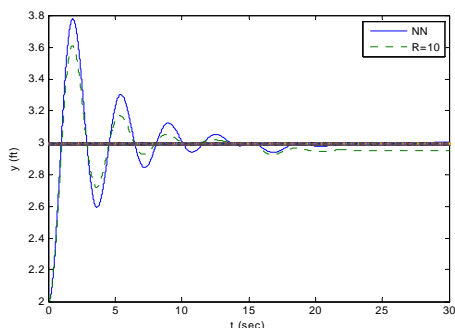


Fig. 10. Lateral position of LQR and NN

3.2 Load is  $5000\text{ lb} \cdot \text{ft}/\text{sec}^2(691.2864\text{N})$

Now the load has been increased to  $5000\text{ lb} \cdot \text{ft}/\text{sec}^2$  after 15 seconds.

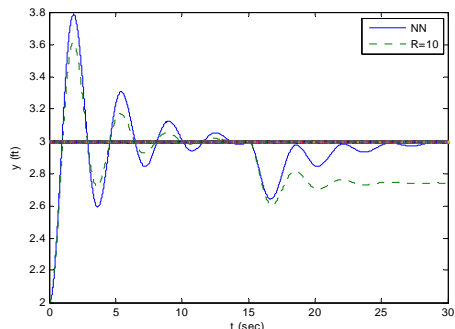


Fig. 11. Lateral position of LQR and NN

We see from Fig. 11 that the neural network controller outperforms in tracking

performance while the LQR controller cannot recover from an error deviation.

## VI. Conclusion

This paper presents tracking control of lateral position of the autonomous four wheel steered vehicle. LQR controllers are designed based on a linearized model. The neural network controller is introduced to minimize tracking errors due to disturbance. Simulation studies show that the neural network controller outperforms LQR controller under present load conditions. A four wheel steered vehicle performs better than two wheel steered vehicle specially when load is present.

## References

- [1] T. A. Lasky and B. Ravani, "Sensor based path planning and motion control for a robotic system for roadway crack tracking", *IEEE Trans. On Control Systems Technology*, Vol.8, No.4, pp. 609-622, 2000.
- [2] H. T. Cho, P. W. Jeon, and S. Jung, "Implementation and control of a roadway crack tracking mobile robot with force regulation", *IEEE Conf. On Robotics and Automations*, pp. 2444-2449, 2004.
- [3] R. T. O'Brien, P. A. Iglesias, and T. J. Urban, "Vehicle lateral control for automated highway systems", *IEEE Trans. On Control Systems Technology*, pp. 266-273, 1996.
- [4] S. Y. Yang, S. T. Park, J. H. Jeong, B. R. Park, "Development of intelligent automated driving control system (lateral control)", *KORUS'99*, pp. 334-337, 1999.
- [5] S. J. Hong, J. Y. Choi, Y. I. Jeong, K. Y. Jeong, M. H. Lee, K. T. Park, K. S. Yoon, and N. S. Hur, "Lateral control of autonomous vehicle by yaw rate feedback", *IEEE Symposium on Industrial Electronics*, pp. 1472-1476, 2001.
- [6] R. H. Byrne, C. T. Abdallah, and P. Dorato,

"Experimental results in robust lateral control of highway vehicles", *IEEE Control Systems Magazine*, pp. 70-76, 1997.

- [7] O. Pages, A. E. Hajjaji, R. Ordonez, "  $H_{\infty}$  tracking for fuzzy systems with an application to four steering of vehicles", *IEEE Conf. On Man and Cybernetics* , pp. 4364-4369, 2003.
- [8] A. B. Will, M. C. Teixeira, and S. H. Zak, "Four wheel steering control system design using fuzzy models", *IEEE Conf. On Control Applications*, pp. 73-78, 1997.
- [9] L. Cai, A. B. Rad, and K. Y. Cai, "A robust fuzzy PD controller for automatic steering control of autonomous vehicles", *IEEE Conf. On Fuzzy Systems*, pp. 549-554, 2003.
- [10] S. Jung and T. C. Hsia, "Neural network inverse control techniques for PD controlled robot manipulator", *ROBOTICA*, pp. 305-314, Vol.19, No.3, 2000.
- [11] H. Miyamoto, K. Kawato, T. Setoyama, and R. Suzuki, "Feedback error learning neural network for trajectory control for of a robotic manipulator", *Neural Networks*, Vol.1, pp. 251-265, 1988.
- [12] S. S. Kim and S. Jung, "Hardware implementation of a real time neural network controller with a DSP and an FPGA", *IEEE Conf. On Robotics and Automations*, pp. 4639-4644, 2003.
- [13] H. T. Cho and S. Jung, "Balancing and position control of an inverted pendulum on an X-Y plane using decentralized neural networks", *Proceedings of the 2003 International Conference on Advanced Intelligent Mechatronics*, pp. 181- 186, 2003.
- [14] J. Y. Wong, "Theory of ground vehicles", *John Wiley & Sons*, 1978.
- [15] S. H. Yu and J. J. Moskwa, "A Global approach to vehicle control: coordination of four wheel steering and wheel torques", *Journal of Dynamic Systems, Measurement, and Control*, Vol.116, pp. 659-667, 1994.

## BIOGRAPHY

### Seul Jung



Dr. Jung received B.S degree in Electrical & Computer Engineering from Wayne State University, USA in 1988.

He received M.S and Ph. D. degree in both Electrical & Computer Engineering from University of California, Davis, 1991 and 1996, respectively. He is currently a professor at Mechatronics Engineering Department, Chungnam National University, Korea.

Research Interests : Intelligent mechatronics systems, creative robot design, human oriented robots, robot education.

Email : jungs@cnu.ac.kr

### T. C. Hsia



Dr. T. C. Steve Hsia received the B.S. degree from National Taiwan University and the Ph.D. degree from Purdue University, both in Electrical Engineering.

Dr. Hsia has been a Professor in the Department of Electrical and Computer Engineering at the University of California at Davis from 1965 to 2001, and a Professor Emeritus since 2001. Dr. Hsia has been a very active member in the IEEE Robotics and Automation Society. He has served as General Chair of IEEE ICRA'91. Dr. Hsia is an IEEE Fellow and the recipient of the IEEE Third Millennium Medal.

Email : tcshsia@gmail.com